D. Cevasco[1]
Ramboll Energy, Wind, Germany Consulting,
Hamburg 22763, Germany;
Department of Naval Architecture,
Ocean and Marine Engineering,
University of Strathclyde,
Glasgow G4 0LZ, UK
e-mails: debora.cevasco@ramboll.com;
debora.cevasco@strath.ac.uk

J. Tautz-Weinert
Ramboll Energy, Wind, Germany Consulting,
Hamburg 22763, Germany
e-mail: jannis.tautz-weinert@ramboll.com

M. Richmond
DNV Energy Systems,
New Taipei City, Taiwan;
Department of Naval Architecture,
Ocean and Marine Engineering,
University of Strathclyde,
Glasgow G4 0LZ, UK
e-mail: mark.richmond@strath.ac.uk

A. Sobey
Maritime Engineering Group,
University of Southampton,
Southampton SO16 7QF, UK;
Marine and Maritime Group,
Data-Centric Engineering,
The Alan Turing Institute,
The British Library,
London NW1 2DB, UK
e-mail: ajs502@soton.ac.uk

A. J. Kolios
Department of Naval Architecture,
Ocean, and Marine Engineering,
University of Strathclyde,
Glasgow G4 0LZ, UK
e-mail: athanasios.kolios@strath.ac.uk

A Damage Detection and Location Scheme for Offshore Wind Turbine Jacket Structures Based on Global Modal Properties

Structural failures of offshore wind substructures might be less likely than failures of other equipments of the offshore wind turbines, but they pose a high risk due to the possibility of catastrophic consequences. Significant costs are linked to offshore operations, like inspections and maintenance activities, thus remote monitoring shows promise for a cost-efficient structural integrity management. This work aims to investigate the feasibility of a two-level detection, in terms of anomaly identification and location, in the jacket support structure of an offshore wind turbine. A monitoring scheme is suggested by basing the detection on a database of simulated modal properties of the structure for different failure scenarios. The detection model identifies the correct anomaly based on three types of modal indicators, namely, natural frequency, the modal assurance criterion between mode shapes, and the modal flexibility variation. The supervised Fisher's linear discriminant analysis is applied to transform the modal indicators to maximize the separability of several scenarios. A fuzzy clustering algorithm is then trained to predict the membership of new data to each of the scenarios in the database. In a case study, extreme scour phenomena and jacket members' integrity loss are simulated, together with variations of the structural dynamics for environmental and operating conditions. Cross-validation is used to select the best hyperparameters, and the effectiveness of the clustering is validated with slight variations of the environmental conditions. The results prove that it is feasible to detect and locate the simulated scenarios via the global monitoring of an offshore wind jacket structure. [DOI: 10.1115/1.4053659]

1 Introduction

The increasing need for reduced operation and maintenance costs has led to focused research on monitoring concepts and frameworks for assessing the health status of wind turbine generator (WTG) systems [1]. Based on the different reliability levels [2], much focus has been on drivetrain components and the electronics of the control systems [1,3–6]. With regard to structural failures, the damage to the turbines' blades are relatively common in the offshore environment [7]. Concerning offshore WTG's tower and foundation, although structural failures are relatively unlikely due to design conservatism, their presence could result in dramatic consequences if undetected [8]. It might also not always be possible to design the support structure in an inspection-free manner; thus, it is sometimes necessary to perform potentially expensive inspection activities during its lifetime. The ability to detect and reliably monitor structural anomalies and failures can have a huge impact on the maintenance costs and on the decision-making of lifetime extension strategies [9].

1.1 Monitoring of Offshore Wind Structures.

To date, a good variety of sensing devices and several analysis methods can be implemented for the structural health monitoring (SHM) of engineering structures [10,11]. Following the classification suggested by [12], the potential SHM approaches are:

- local monitoring, aimed at direct measurements and strongly dependent on the monitored structure;
- global—also called vibration-based—monitoring, for the indirect detection of deviations in the response of the system, and applicable to any type of structure.

Local monitoring strategies for WTGs can include, for instance, the use of strain gauges for the direct monitoring of fatigue damage, the installation of sonar sensors for the monitoring of the scour phenomena, but also nondestructive test evaluations to be performed on-site [12]. Although the postprocessing of the measured signals, for the detection of anomalies, is relatively

[1]Corresponding author.

Manuscript received March 15, 2021; final manuscript received January 14, 2022; published online March 7, 2022. Assoc. Editor: Imad Abdallah.

straightforward, the cost of these sensors' installation and maintenance, and/or performing a visit to the WTG, is generally high for offshore applications [13]. In contrast, the use of vibrational data for the monitoring of the offshore structure's global dynamics is relatively cheaper and more flexible. However, when relying on vibrational data, the detection of anomalies is challenged by the fact that:

- the recording of changes in the dynamic behavior is potentially associated with several factors and/or coexisting modes of failure of the structure [13],
- the application of output-only modal analysis on operational systems in nonstationary conditions [14]—so-called operational modal analysis (OMA)—to derive the system's modal properties, has some intrinsic uncertainties.

For the detection of damage in offshore wind structures (see following Sec. 1.2), the monitoring methods based on the derivation and the tracking of modal properties—i.e., parametric damage detection methods –, have been the prime focus of research. Data normalization and clustering approaches are generally applied on the OMA results to reduce the effect of operational conditions [15,16]. Other authors proposed unconventional methods to improve the accuracy of the identification results: Dong et al. [17,18] investigated a modified stochastic subspace system identification, while Tcherniak and Larsen [19] suggested the use of data from the blades to improve the observability of aerodynamically damped global modes.

1.2 Vibration-Based Damage Detection of Wind Turbines and Offshore Structures. Global monitoring and parametric-based detection methods have been already employed to some offshore wind full-scale case studies. Weijtjens et al. proposed a data-driven SHM framework in Refs. [20,21]. Their approach consists of tracking the system modal properties according to the different operational conditions (i.e., parked and operating case) then subgrouped according to RPM and pitch ranges. They then normalized the variability of each mode of vibration, by using a nonlinear regression model. In Ref. [30], they observed that some of the modes correlate to environmental effects such as the seawater temperature—especially for low order modes –, the tidal level, and the water height, besides being dependent on the yaw angle for asymmetry of the structure. In Ref. [21] they additionally recognized changes in the vibration levels of the tower top accelerometer depending on the wind farm wake effect. Finally, by detrending the OMA results based on the environmental fluctuations, they managed to recognize the stiffening of the response of a turbine installed on a monopile foundation [20]. A similar approach was followed by Oliveira [22] to identify the presence of numerically simulated damage in the foundations (crack and scour), and blades (uniform deterioration due to operation). These monitoring methods, based on the use of the control chart theory [23], allow for the damage detection only (level I, as defined in Ref. [24]). More advanced machine and deep learning algorithms might be preferred to capture complex patter in the data [12]. If interested in identifying the location of the damage and assessing it (levels II and III, respectively, as defined in Ref. [24]), the models to deploy typically require a structure that accounts for interdependencies between the sensing points, as studied in Refs. [25,26].

However, data-driven methods are conditioned by the significance of historical data. For this reason, several authors made use of models to simulate representative datasets for the healthy and damaged system dynamics. In Ref. [27], Nguyen et al. numerically investigated the feasibility of vibration-based damage assessment for an offshore WTG with gravity-based foundation, excited by various waves loads. In Ref. [28], Richmond et al. conducted a sensitivity study on the changes in the dynamic response of an offshore wind jacket structure, for several sources of anomaly and by ranging their severity. In Ref. [29], Nguyen et al. proposed the use of a vibration-based artificial neural network for the estimation of location and severity of simulated structural damage in onshore WTG towers. The main findings outlined that a detection algorithm trained on frequencies only performed better for the assessment of the severity.

In terms of indicators of the damage, the modal curvatures have been extensively investigated for experimental and numerical studies of beam- and plate-like structures [30,31]. Therefore, in the context of civil engineering for the wind energy sector, curvature-based methods found an application for the detection of blades damage mainly [32,33]. However, as concerns the monitoring of the global modal properties of a wind turbine structure, Richmond et al. [28] argued that the detection via the mode curvature could be challenged by the generally limited amount of sensors installed.

Extensive research was also conducted for the detection of structural failures in offshore (oil and gas) jacket platforms. Liu et al. [34] suggested a modal flexibility-based method using a finite element (FE) model updating technique. Modal flexibility detection approaches belong to a family of traditional vibration-based methods, together with frequency-based and mode shape ones [35]. The modal flexibility is influenced by the low-order modes mainly, being thus suitable for the offshore wind SHM applications, where higher modes are generally difficult to extract. Liu et al. applied a gradient-based method for the minimization of the Frobenius norm of the matrix representing the residual of the flexibility between the damage condition and a healthy reference (cf. [12] and Sec. 2.2). Another model updating approach applied to an offshore truss structure was proposed by Malekzehtab and Golafshani in Ref. [36]. For their updating procedure they applied a genetic algorithm to optimize a cost function defined as the sum of the distances between the frequencies and of the mode shapes between the reference and the damaged conditions. In both Refs. [34] and [36], the algorithms successfully identified the damages' location and severity, additionally accommodating measurement uncertainties and several noise levels. Regarding the application of machine learning methods, Xu et al. [37] used a residual strain energy method and employed principal component analysis to remove the influence of the environmental temperature variation. Concerning the nonparametric vibration-based methods, it is worth mentioning the work of Diao et al. [38] and Cheng and Wang [39] as applied to offshore platform structures.

1.3 Aim and Objectives. This works aims to develop a damage detection and location scheme for offshore wind jacket structures, combining data-driven and model-based detection approaches. Fully data-driven methods rely on a representative set of data for building up a digital twin of the structure's normal behavior. On the other side, model-based methods, requiring the availability of a comprehensive model of the structure, allow to simulate the effect of rare events for which data are usually unavailable.

A monitoring scheme is deemed suitable for industrial needs if the following criteria are achieved: (i) detecting and distinguishing anomalies of different causes, (ii) use of low-cost measurement technologies, (iii) transparency of the reasoning process—versus black-box models, (iv) use of a probabilistic approach for the decision making, and (v) enabling a real-time monitoring. The strategy, as presented in Sec. 2, is to employ modal simulated data from a FE model of the WTG structure—which underwent a data-driven model updating -, to instruct data-based monitoring algorithms to identify and locate the damage. As the feasibility of the suggested approach is the main concern of this work, the investigation is limited here to the turbine idling state for simplicity.

Starting from the findings of Ref. [28], six types of localized structural damage and several levels of scour are simulated for the case study presented in Sec. 3. The feasibility of the detection is discussed in Sec. 4, together with a consideration of the set of features to derive and track. Finally, in Sec. 5, the limitations of the

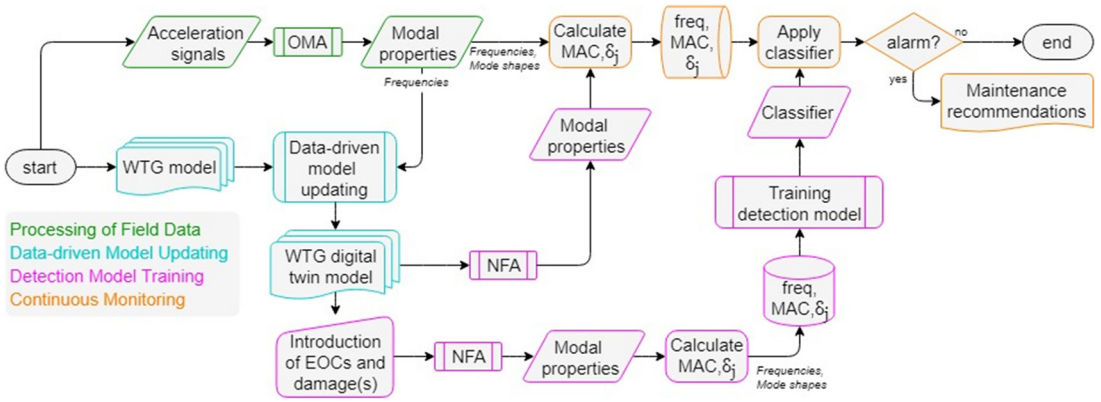

Fig. 1 Processes and data flow for the suggested monitoring strategy

current approach, and the challenges prior its field application, are outlined.

2 Methodology

The flow of data and processes for the field application of this monitoring approach is given in Sec. 2.1. In Sec. 2.2, details are provided on the simulation setup to extract the modal properties of the structure and calculate their deviations. The machine learning algorithms and the processes for their training, testing and validation are presented in Sec. 2.3.

2.1 Monitoring Approach. An overview of the workflow for the suggested structural health monitoring and damage detection scheme is given in Fig. 1. The pillar of this strategy is the model-based digital twin technology [40–42]. Passing through the screening and diagnostics of the structure (level 1), the FE model updating (level 2), the load calibration (level 3), and the quantification of the uncertainties (level 4), a digital twin model can finally be employed to continuously monitor the accumulated fatigue damage in the hot spots of the structure (level 5). For the purpose of the identification of the damage and its location, a level 2 digital twin is deemed sufficient.

The application of a data-driven model updating procedure is presented by Augustyn et al. in Ref. [43]. They calibrate the FE model parameters to match the structure's measured global modal properties as close as possible to reality. This twinning process is meant to reduce the numerical model's uncertainties related to the manufacturing (e.g., joint stiffness and masses) and the installation (e.g., soil properties and tolerances) processes.

The modal properties of the system in its normal behavior—depending on the environmental and operational conditions—and in its damaged status, are retrieved from natural frequency analysis simulations. By comparing the extracted modal properties with those of a reference healthy scenario, modal indicators, such as the modal assurance criteria (MAC) and the modal flexibility variation (δ_j), are calculated and employed to track the system's dynamics evolution and deviation. This set of information, stored into a database, is used for instructing detection models to identify and locate (detection levels I and II) the system's anomalies. The instructed algorithms can then be used on the modal data derived from the field vibrational data, to raise alarms if the pattern of one of the simulated damage scenarios is recognized.

In contrast to the approaches of Refs. [34] and [36], where a further model updating is used to detect location and severity (level III) of the damage, a classification-based detection is suggested here. The reason for this decision is related to the fact that, for offshore wind applications, several types of damage are potentially critical for the substructure. The approach proposed can easily be extended to setup the detection of anomalies of every type, while the studies in Refs. [34,36] find their application for the detection of damage controlled by a single model parameter—, e.g., elements' and joints' stiffness. Additionally, the uncertainty of the simulated data is introduced by a slight variation of the environmental parameters (e.g., scour and tidal phenomena), rather that adding several levels of white noise to the signals.

2.2 Data Acquisition. The study of the dynamics of the WTG structure in its healthy conditions, and in response to anomalies in the system, is obtained via the natural frequency analysis of an FE-updated model, setup in the ROSAP (Ramboll Offshore Structural Analysis Package) software. This implementation does not allow the integration of moving and/or rotating parts, and thus represents only the WTG dynamics in idling condition. The rotor-nacelle-assembly is, however, integrated for its contribution in terms of mass and inertia. It is worth mentioning that, the methodology suggested can be applied independently of the type of software used for the analysis. However, if the modes extraction is carried out via an aero-hydroservo-elastic tool, it would be possible to extend the analyses to account for the interference of the rotor dynamics and the effect of the different WTG operating regimes.

The eigenfrequencies and their corresponding mode shape vectors are derived for several integrity scenarios of the WTG jacket and for varying environmental conditions. After selecting a healthy reference scenario, the indicators introduced in Secs. 2.2.1 and 2.2.2 can be calculated.

2.2.1 Modal Assurance Criterion. The MAC provide a comparative value between two vectors, giving a measure of their level of consistency. A value closer to 1 means that the vectors are consistent and a value at or close to 0 means that the vectors are inconsistent. MAC are calculated between two modal vectors (e.g., $\{\phi_r\}$ and $\{\varphi_s\}$), according to the following equation [44]

$$\mathrm{MAC}(\{\phi_r\},\{\phi_s\}) = \frac{|\{\phi_r\}^T\{\phi_s\}|^2}{(\{\phi_r\}^T\{\phi_r\})(\{\phi_s\}^T\{\phi_s\})} \tag{1}$$

2.2.2 Modal Flexibility Variation Per Sensor Location. The modal flexibility matrix ([F]) is derived according to Eq. (2), with n being the number of measured modes. In the calculation of the [F], the mode shape matrix $[\Phi]$, with $\{\phi_i\}$ being the mode shape vector of the i-th mode, is weighted by the diagonal matrix of rigidity $[\Omega]$, corresponding to $[\omega_i^2]$ where ω_i is the i-th frequency. Each column of [F] represents the displacement pattern of the structure associated with a unit force applied to each degree-of-freedom (DOF) of the structure

$$[\mathrm{F}] = [\Phi][\Omega]^{-1}[\Phi]^T = \sum_{i=1}^{n} \frac{1}{\omega_i^2}\{\phi_i\}\{\phi_i\}^T \tag{2}$$

The residual matrix of the modal flexibility ([ΔF]) is measured by calculating the flexibility matrices before and after the damage ([F*]) and subtracting them, as in Eq. (3)

$$[\Delta F] = [F*] - [F] \tag{3}$$

The absolute maximum of each j-th column of the $[\Delta F]$—as for Eq. (4)—is the modal flexibility variation in each DOF ($\bar{\delta}_j$). It indicates where the maximum variation in flexibility is produced. This quantity has been historically used to estimate changes in the static behavior of the structure from the dynamically measured modal properties of the system [45]

$$\bar{\delta}_j = \max|\delta_{ij}| \quad \text{for} \quad i,j = [1, n] \tag{4}$$

2.3 Machine Learning Processes and Algorithms. This section introduces to the selected machine learning algorithms and features, by explaining the criteria and the decision-making process behind their selection. Finally, the processes for the training and testing of the detection models and their validation is detailed.

2.3.1 Selection of the Features. For the investigation of this paper, three sets of features are analyzed: a set of frequencies only, a set consisting of frequencies and MAC values, and a set including frequencies and $\bar{\delta}_j$. Frequencies, rather than relative difference of frequencies, are selected and normalized, together with other possible features, during the preprocessing phase. By adding the MAC values, the algorithm is also informed on the deviation of the shapes of vibration. Being used as a indicator of the goodness of the extracted modes during the postprocessing of the OMA results, it can happen that modes with a low MAC value get filtered out of the analysis, although potentially signaling the presence of damage. An alternative measure of the modes' deviation can be given by the $\bar{\delta}_j$, which additionally provides a higher level of information because of being not only sensitive to the mode, but also to the sensor location.

2.3.2 Selection of the Algorithms. Allowing data samples to belong to two or more class types, with different levels of membership, is the main criterion for the selection of the detection algorithms to be tested in this feasibility analysis. This requirement reduces the choice to soft-classification models, to explicitly estimate the class conditional probabilities, and discards the more complex-to-interpret deep learning and tree-based models. Either fuzzy- or Bayesian-based models inform on the degree of membership of each data sample to the given classes. Targeting a multiclass classification, a predictive model based on the linear discriminant analysis (LDA) theory is deemed more suitable than setting-up multiclass logistic regression models. However, the particular set of data in analysis violates the LDA assumptions of normally distributed data and identical covariance matrices for every class [46]. For this reason, fuzzy-based models only are investigated further.

Fuzzy logic is an organized and mathematical approach, able to handle inherently imprecise concepts through the use of membership functions. In their simplest application, these functions are manually defined setting the truth values, and a set of fuzzy rules is given to describe how one or more fuzzy variables relate to another. Although such a transparent approach would be preferred, the mapping by hand of variables and rules is not straightforward for the targeted application. Therefore, the fuzzy logic principles are automatically applied to cluster the multidimensional data, according to the so-called fuzzy c-means (FCM) method [47]. The algorithm works by assigning membership to each data point corresponding to each cluster center on the basis of distance between the cluster and the data point. This unsupervised method is controlled by specifying the number of clusters to identify, the fuzzy exponent and a termination tolerance [48].

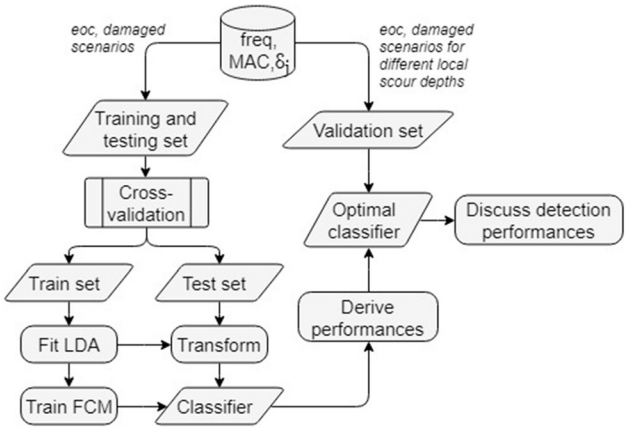

Fig. 2 Processes and data flow for training, testing, and validating the detection algorithms

Specifically, the Python open-source version of [49] is used for the purpose of this paper.

2.3.3 Training, Testing, and Validation Processes. A sketch of the flow of data and processes for the training, testing and validation of the FCM model is given in Fig. 2. The cross-validation procedure [50] is employed to verify the independency of the prediction on the WTG operating condition (yaw angle rotation). Although the supervised LDA was not considered suitable for the application, Fisher's LDA reduction technique is applied, by transforming the set of features while maximizing the separability of the classes. As investigated by Li et al. [46], the LDA for dimensionality reduction can also work reasonably well if those assumptions are violated. Based on the optimal rotation and the reduced features found in the training set, the datasets for testing and validation are consequently transformed. Multiple FCM models are then trained during the cross-validation process, assigning each data sample a membership to each cluster center. Only the best performing models—one for each set of feature combinations—are tested on the validation dataset. To discuss the detection capability of the algorithms, hard-threshold metrics are used—by allocating to each data sample the label according to the highest membership predicted.

3 Case Study

The structure being analyzed in this study is an Adwen AD-5 MW installed on a 4-legged jacket as the support structure. This turbine sits in the 350 MW Wikinger wind farm, located in the German exclusive economic zone of the Baltic Sea. The water depth at the turbine specific location is approximately 38 m, at the mean sea level. The pile penetration depth is approximately 30 m beneath the seabed, which mainly consists of cohesive clay.

3.1 Wind Turbine Generator Measurements and Finite Element Model. The chosen wind turbine belongs to the 10% of the structures with an SHM system installed. The setup of the monitoring systems, and the sensors' and the elements' naming conventions are illustrated in Fig. 3. As it is generally recommended for offshore WTG structures [51], the accelerometers are installed at 4 levels, including the tower-top (section A-A), around the midtower (section B-B), the tower base (section C-C), and jacket base (section D-D). These consist of a set of four triaxial accelerometers, at each leg of the transition piece, and three biaxial accelerometers, along the tower sections. This sensor configuration aims to extract the first five global dynamic modes of the structures, consisting of the 1st and 2nd global bending modes of the tower, both in fore-aft (FA) and side-side directions, and the 1st torsional mode of the support structure.

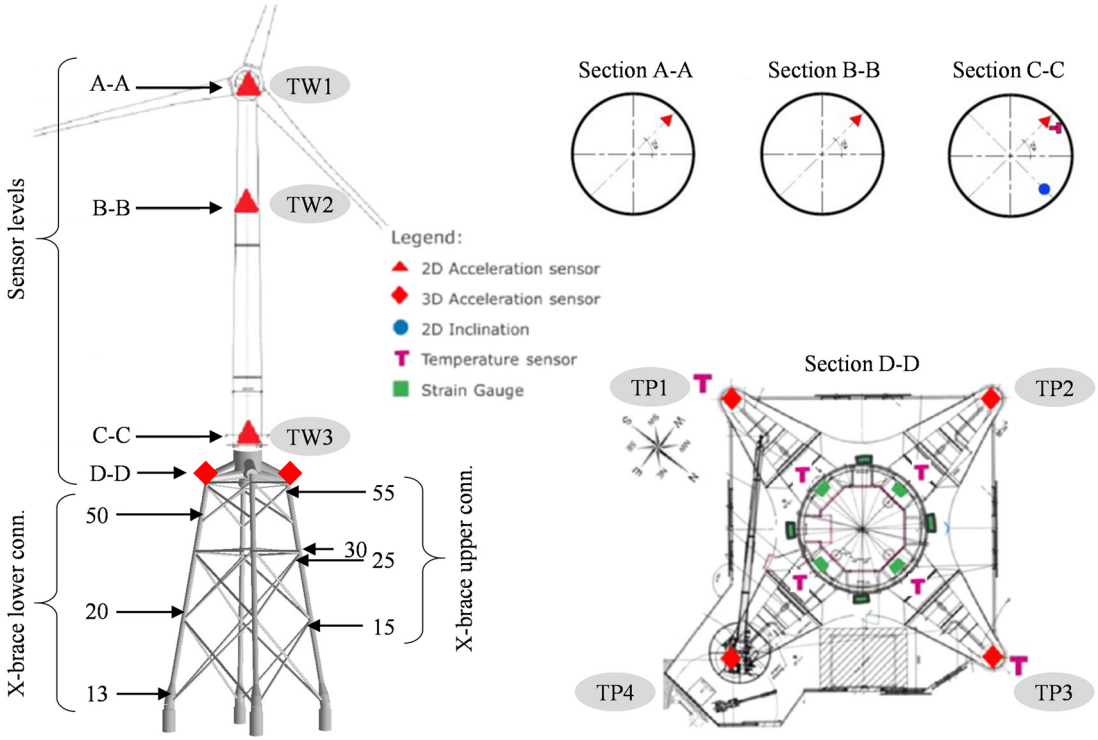

Fig. 3 Wind turbine geometry and SHM system. The *x* and *y* axes are oriented along north and west directions, respectively.

Based on these measurement data, together with information from the 10-min SCADA data on the turbine's operating condition, Augustyn et al. [43] updated the FE model of the WTG to match at best the real system dynamics in its as-installed condition. After the update, the discrepancy between the measured and modeled global frequency is reduced as follows: from the initial design discrepancy of 6% to 0.3% for the 1st tower modes, and from 30% to 1.0% for the second tower modes. Furthermore, the MAC values with respect to the measured mode shapes generally improved after the update, reaching a value of 0.99 for the second FA mode from the initial 0.85 of the design. Although the first torsional mode of the jacket was not used for this model calibration, it will be included in the following analysis to investigate whether its monitoring is beneficial for detection purposes.

3.2 Simulation of the Scenarios. Scenarios for the healthy and the damaged status are simulated on the FE-updated WTG model described in Sec. 3.1. Given that, from the design specification, the site accounts for only a few centimeters of variation in the water level for tidal phenomena, the measurements' uncertainty is introduced solely by varying the local scour depth within the design limit. In regard to the operating regimes, idling-only conditions are mimicked, accounting for the impact of the rotor-nacelle-assembly yawing on this asymmetric system inertia, and thus on its modal properties.

The damage scenarios are simulated following the recommendations of Scheu et al. [8]. They prioritized the following failure modes for an offshore wind substructure: excessive corrosion, fatigue, deformation and buckling, grout connection and bolted connection. As the design of this WTG substructure is fatigue-driven, extreme scour events can be of concern for fatigue damage [52], bringing the utilization of the jacket structure outside the design assumptions. For this reason, the impact of the scour phenomena is analyzed in Sec. 3.2.1. Additionally, as a consequence of decisions taken in the design phase, the monitoring of critical welds and joints could be expected for the preventive detection of cracks. These inspections can be required for elements above—especially in the splash-zone—or even below the water level, increasing for the latter the cost for their visual examination. The detectability of jackets' members integrity loss is discussed in Sec. 3.2.2.

3.2.1 Scour. The scour phenomenon is the process of the removal of sediment from around the turbine foundations. The seabed being carried away by hydrodynamic action can either result in the reduction of the soil around the whole area of the foundation (global scour) or solely the area at the structure piles (local scour). The FE model includes details of multiple soil layers and so when a scour depth is introduced, the top soil layers are removed. The removal of the weight of the top layers is associated with a variation in the soil stiffness. However, by updating the force-displacements curve, it was noticed that this variation has only a minor effect on the structure dynamics, affecting mainly the loading in a downward direction. Thus, it is considered a good assumption for this analysis to refer to the force–displacement curves used for the design. The global scour phenomenon, which would impact the soil stiffness the most, is generally considered in the case of noncohesive soil. The cohesive clay soil of the Wikinger wind farm, is primarily affected by a local scour phenomenon. A design limit of 2.2 m scour erosion is given for the turbine location being analyzed.

In Fig. 4, the local scour depth ranges from 0 m to a value of 3.2 m, uniformly for all the legs, and by keeping the scour angle constant at 18 deg, as assumed from the design. The design limit value is reported in the figure with a cross symbol; this identifies the maximum fluctuation of the estimated metrics in the normal state of the structure for a fixed nacelle angle.

The reference for estimating the metrics of Fig. 4 is taken with respect to the no-scour scenario. It is evident that the tower's second bending modes are the ones mainly affected by the scour depth increase. However, the variation mainly affects their frequencies—with a drop of about 4% for the second FA mode at 3.2 m scour –, while their mode shapes are almost unchanged—with MAC values higher than 0.99. In addition, it is worth pointing out that, in the case of the presence of local scour, a higher $\bar{\delta}_j$ is recorded by the tower's top sensors.

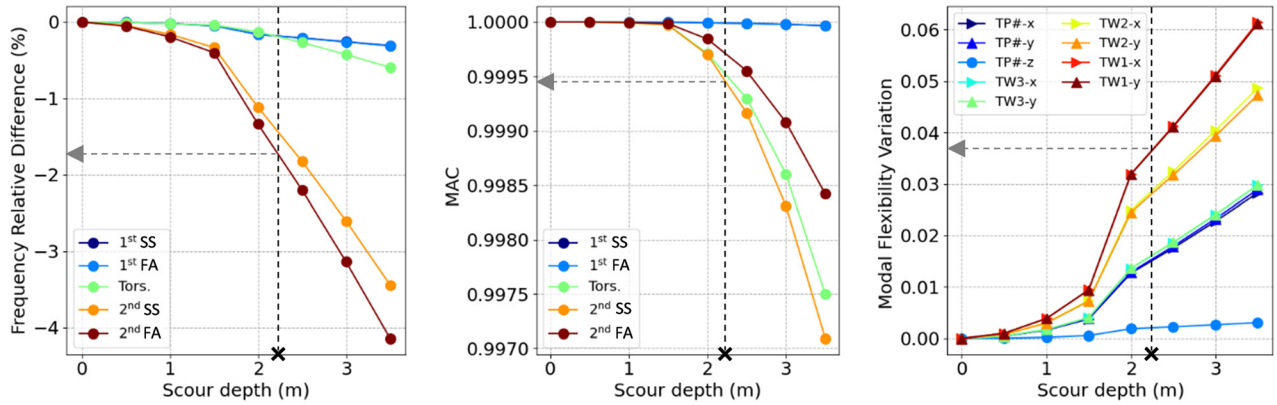

Fig. 4 Dynamic properties variation for developing local scour phenomena

3.2.2 Loss of Structural Integrity in the Brace Elements. The localized structural damage is implemented in the ROSAP model of the substructure by varying the Young's modulus (E) of its elements and subelements. The damage types that could be associated with a variation in stiffness of the structural members of the jacket are corrosion, material softening due to cyclic loading, and loosening of the connection between elements. The simulation of the full integrity loss of the jacket leg would not lead to representative results, due to the fact that either full or partial integrity of the legs is required for the substructure's survivability. In contrast, it was observed that the substructure might survive the loss of integrity of the brace members.

In Fig. 5, the E of each of the brace elements of the jacket structure connecting to a leg element is reduced to 1% of the design value. The results are reported with respect to the several levels of Fig. 3, and in terms of the relative difference in frequency, the MAC values, and the $\bar{\delta}_j$. For each brace level, eight values are reported, corresponding to the eight brace-to-leg connections, two per leg, of this 4-legged jacket structure. Because of this, and due to the fact that the results in Fig. 5 are relative only to a single rotor-nacelle-assembly position, it is possible to observe some analogies in the results at each level, with slight differences that are caused by the damage locations and system's asymmetry between the legs. By reporting the thresholds identified in Figs. 4 to 5 (light gray shaded areas), it is evident that the ranges of variability due to the environmental and operational condition overlap with the deviations caused by the structural failures, emphasizing how this poses a challenge on damage detection and location.

In general, it can be observed in Fig. 5(*a*), that the frequencies of the 1st torsional mode and the 2nd tower modes are mainly affected by the presence of the disconnection. These modes grow in difference with respect to the reference healthy scenario—almost up to 2.5% for the 1st torsional mode—if the damage is closer to the splash-zone, and thus to the sensorized area of the WTG jacket—cf. Figure 5(*b*). The changes in the mode shapes, shown in Fig. 5(*b*), concern mainly the 2nd side-side mode for the lower brace level. The 1st torsional mode consistency declines in the case of damage to the higher brace levels, scoring a MAC value as low as 0.88 at level 55. Concerning the $\bar{\delta}_j$ of Fig. 5(*c*), it can be noticed that the sensors located in the transition piece are the ones recording the highest variation, with alternating direction and sensors positioning, depending on the leg where the damage is implemented. Only a few damage locations, and for heights above level 20, impact the flexibility recorded by the sensor located at the tower top. It is finally interesting to observe that the presence of structural damage in the horizontal elements of the jacket (level 30) cannot be detected by any of the modal global modes. For this reason, the detection of these damage locations will be excluded from the following analysis. Instead, the detection of disconnections at one location per level (13-15-20-25-50-55) is investigated, implementing for simplicity all damages on the same leg and on the same leg-side.

3.3 Training, Testing, and Validation Datasets. The data samples for training, testing, and validating the detection algorithms are simulated, as explained in Sec. 2.2, by introducing the anomalies described in Sec. 3.2. The detection algorithms then try to cluster the data into as many clusters as the number of simulated WTG status, corresponding to the following labels:

- *eoc*, reproducing the structure behavior for local scour depth up to the design threshold,
- *scour*, modeling scour phenomena over the design allowance,
- *D55*, *D50*, *D25*, *D20*, *D15*, and *D13*, mimicking the integrity loss of brace members at the leg K or Y joints, for the levels from 55 to 13, as reported in Fig. 3.

The training and testing phases are used to verify the effectiveness of the clustering of the WTG status for variation in the nacelle position. The training set contains data samples at every yaw angle from 0 to 359 deg, with a 1-deg step, for each of the simulated labels. A ten-fold cross-validation—as presented in Sec. 2.3—is implemented to split in training and testing. The testing results are used to select the best setup of the hyperparameters, in terms of LDA components, and to verify the goodness of the clustering via the fuzzy partition coefficient [49].

The validation of the trained models on data samples, for variation of the scour level, is used to confirm the performances for unseen set of data, and to recommend the best set of modal indicators to be used for the detection task. The validation set contains all simulated labels at every yaw angle from 0 to 359 deg, as for training and testing. However, for each of the simulated labels, the environmental conditions—implemented via the scour depth parameter—are varied. Two different validation sets are investigated, one for a slight variation of the scour depths and one for scour depths approaching the design allowance, respectively.

4 Results and Discussion

This section presents and discusses the results from the LDA transformation and the fuzzy clustering model, which are used to investigate the detectability of anomalies in the system. Although the fuzzy clustering belongs to the so-called soft-clustering methods, the results are mainly reported in terms of threshold metrics [53]. Therefore, a label is assigned to each data sample based on the highest membership predicted by the fuzzy clustering model.

4.1 Training and Testing on the Operational Variations. The focus of this preliminary analysis is on the identification of the optimal number of the LDA transformed component, for the

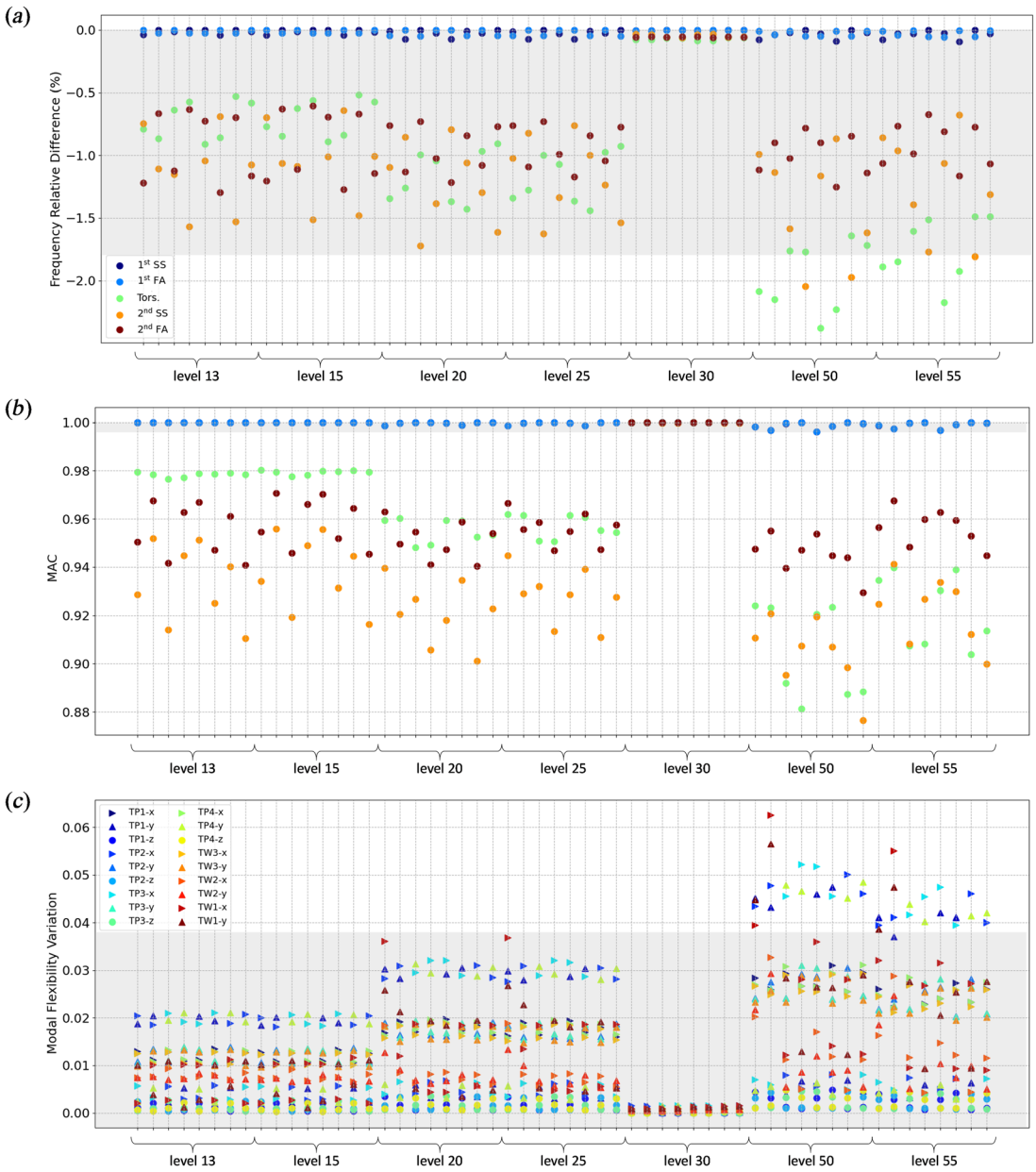

Fig. 5 Dynamic properties variation for the full integrity loss of single brace members: (*a*) frequency relative difference, (*b*) MAC values variation, and (*c*) modal flexibility variation

reduction and rotation of the modal indicators into features separating at best the eight classes. The cross-validated estimates are reported in terms of macro-averages of the accuracy and of the F1-score [53]. The accuracy gives an indication of the total amount of correct predictions over the total amount of samples in the dataset tested. The F1-score is the harmonic mean of the precision—defined as the percentage of correctly detected damaged cases with respect to the total amount of cases predicted to be damaged—and recall—defined as the portion of correctly detected damaged cases with respect to the total amount of damaged cases in the dataset tested. For multiclass classification, the macro-average (arithmetic) of these metrics can be calculated by aggregating the contributions of all classes [53], with c being the number of classes, as indicated in Eq. (5)

$$\text{metric}_{\text{macro}} = \frac{1}{c}\sum_{i=1}^{c}\text{metric}_i \tag{5}$$

The fuzzy clustering models are trained to identify all eight centers on uniform, but randomly selected, subsets of the training set—according to the cross-validation process explained in Sec. 2.3.3. In Fig. 6, the box plots of the fuzzy clustering results, for the three feature combinations, are presented for varying numbers of the LDA components. The random selection of the subsets for this training and testing phase is the reason for the predictions' variance.

It can be observed, in Fig. 6(*a*), that the detection based on the tracking of frequency only has already quite satisfactory performances. The macro-accuracy and F1-score reach median values above 93% and 74%, respectively, by selecting the first two LDA components. Slight improvements—with a median macro-accuracy of about 94% and a median macro-F1-score of 76%—are achieved by including the features relative to the MAC values of the modes. As shown in Fig. 6(*b*), this is achieved by additionally extending the number of LDA components (from three to five). It is finally evident, in Fig. 6(*c*), that the fuzzy

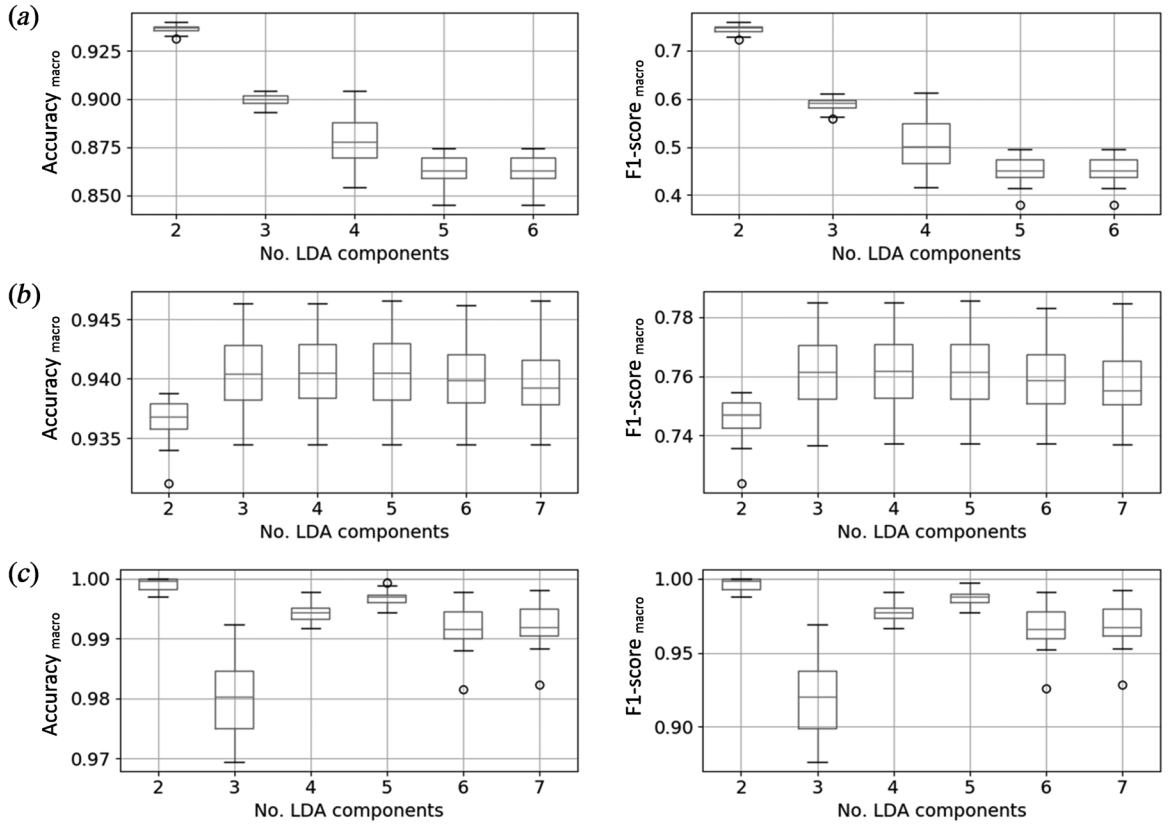

Fig. 6 Macro-average of the metrics from the hard-threshold clustering results for a varying number of LDA components. The algorithms are trained on the following features: (*a*) frequencies only, (*b*) frequencies and MAC values, and (*c*) frequencies and $\bar{\delta}_j$, and tested on subsets of the training set.

Table 1 Summary of the optimal number of LDA-transformed features and estimated metrics on the test set

Input	Total number of features	Optimal no. of LDA features	Accuracy $_{\text{macro}}$ (95% CI)	F1-score $_{\text{macro}}$ (95% CI)
Frequencies	5	2	93.6% ± 0.3%	74.4% ± 1.4%
Frequencies + MAC values	10	5	94.1% ± 0.5%	76.4% ± 1.8%
Frequencies + $\bar{\delta}_j$	23	2	99.8% ± 0.1%	99.5% ± 0.5%

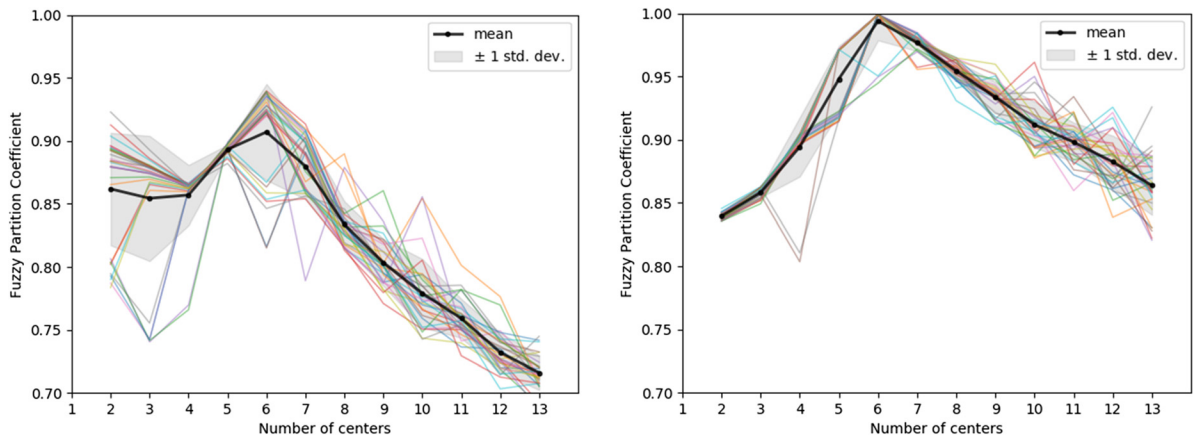

Fig. 7 Fuzzy partition coefficient for a varying number of cluster centers, training the model on the frequencies and MAC values (on the left), or the frequencies and the $\bar{\delta}_j$ (on the right)

clustering models correctly classify the majority of the WTG status, by including the information on the modal flexibility variations. The generally low variability of the prediction indicates the independency of the models of the nacelle position. By accessing the first two LDA components only, macro-accuracies and macro-F1-scores close to 100% are obtained. For each of the features' combinations in analysis, the identified best hyperparameter, the corresponding estimated metrics, and their 95% confidence intervals, are reported in Table 1.

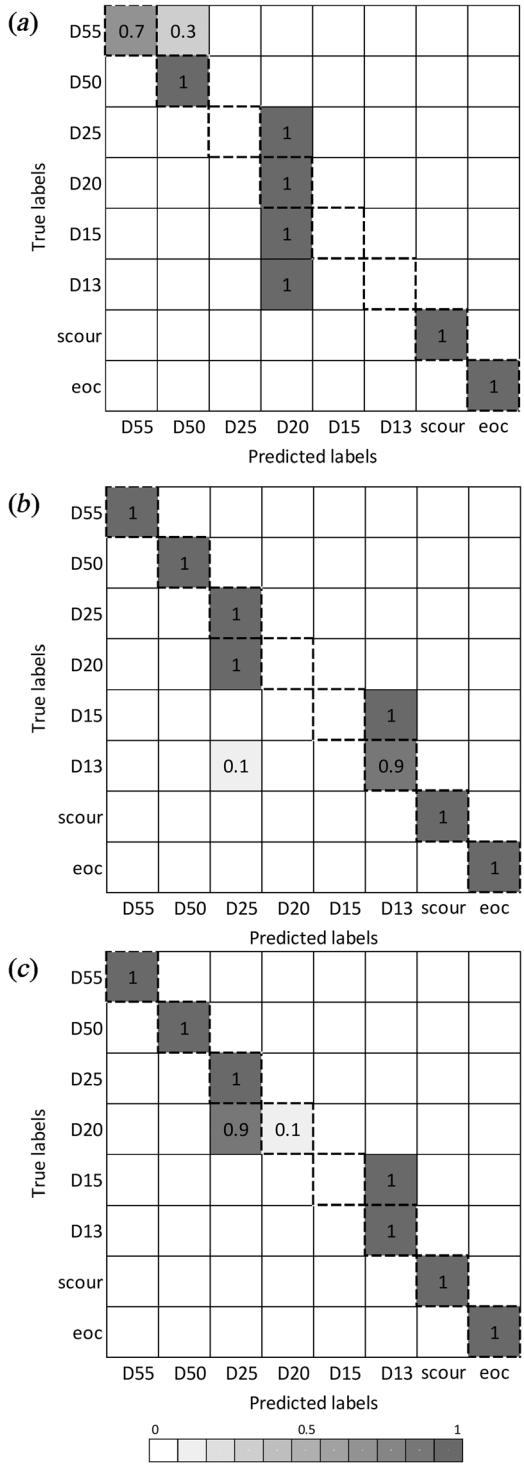

Fig. 8 Confusion matrix of the fuzzy clustering prediction on the validation dataset. Results are reported for the detection models trained on: (*a*) frequencies only, (*b*) frequencies and MAC values, and (*c*) frequencies and $\bar{\delta}_j$.

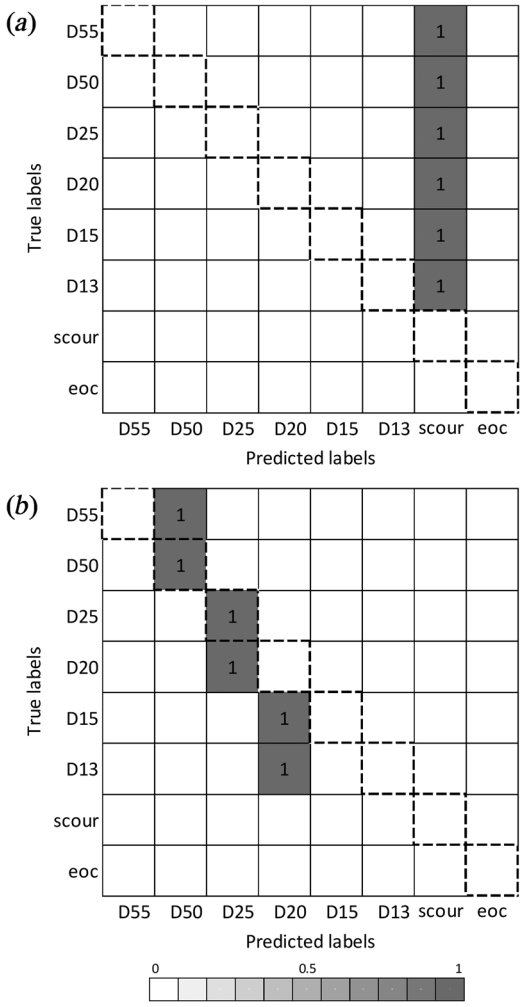

Fig. 9 Confusion matrix of the fuzzy clustering prediction of the dataset for the combination of single brace damage and scour depth approaching the design allowance. Results are reported for the detection models trained on, (*a*) frequencies and MAC values and (*b*) frequencies and $\bar{\delta}_j$.

The goodness of the detection, based on the features' combination including the frequencies and the $\bar{\delta}_j$, can also be observed in the generally high values of the fuzzy partition coefficient of Fig. 7 (right). The coefficient represents how cleanly the data are separated into the selected number of clusters [49]: it ranges from 0 to 1, with 1 being the best separation. The scatter in the results is again given by the training and testing of several models on subsets of the dataset. Although the models do not reach their best performances by clustering into eight groups of behavior—but into six–, it is observable that the detection achieved by using the $\bar{\delta}_j$ generally outperforms the one by using the MAC values, in Fig. 7 (left).

4.2 Validation for the Variation of the Environmental Conditions. Figure 8 shows the performances of the tuned fuzzy clustering models of Sec. 4.1 on the first validation datasets with slightly increased scour depths. The results in Fig. 8 are presented in the form of a confusion matrix. A gray color scale is used to indicate the density of the data sample for each pair of true-predicted labels, with dark gray being 1 (or 100% data samples) and white being 0. The diagonal of the confusion matrix, in dashed lines, represents the correctly labeled predictions, which is supposed to be populated by density 1 (thus in a dark gray color). To ease the interpretability of the results, the validation outcomes are presented here only for the best performing models on the training and testing sets (cf. Fig. 6).

In Fig. 9, the algorithms trained on MAC values and $\bar{\delta}_j$ are further validated on the second validation dataset replicating the brace disconnections, together with higher depths of local scour, yet within the scour allowance. In Fig. 9(*a*), it can be observed that the model relying on frequencies and MAC values transfers all its predictions to the extreme scour scenario. In contrast, the model trained on frequencies and $\bar{\delta}_j$ correctly identified the disconnection damages as such. Nonetheless, as shown in Fig. 9(*b*),

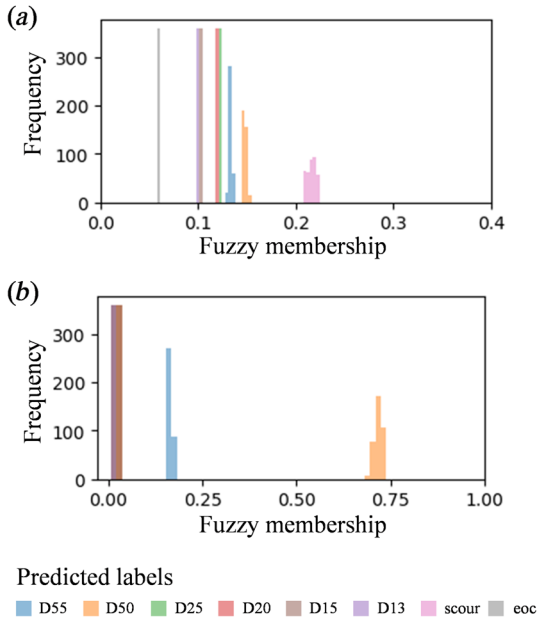

Fig. 10 Histogram of soft clustering membership predictions on the dataset for the combination of single D50 brace damage and scour depth approaching the design allowance. Results are reported for the detection models trained on, (*a*) frequencies and MAC values and (*b*) frequencies and $\bar{\delta}_j$.

the addition of extra scour caused the mislocation of the damage for levels 55, 20, 13, and 15.

To show the benefit of the probabilistic monitoring approach, the membership predictions of the fuzzy clustering are reported in Fig. 10 as histograms of probabilities for case D50 of Fig. 9. It is evident, in Fig. 10(*a*), that the misclassification into extreme scour scenario for the model trained on frequencies and MAC values, is associated with generally low membership to any of the simulated labels. Even if the assigned label—i.e., "scour" —has clearly the highest predicted probability, its value is below 0.3. Concerning the detection via frequencies and $\bar{\delta}_j$, it can be observed, in Fig. 10(*b*), that although the damage scenario D50 has the highest probability, the true scenario label D55 shows a probability higher than the remaining scenarios.

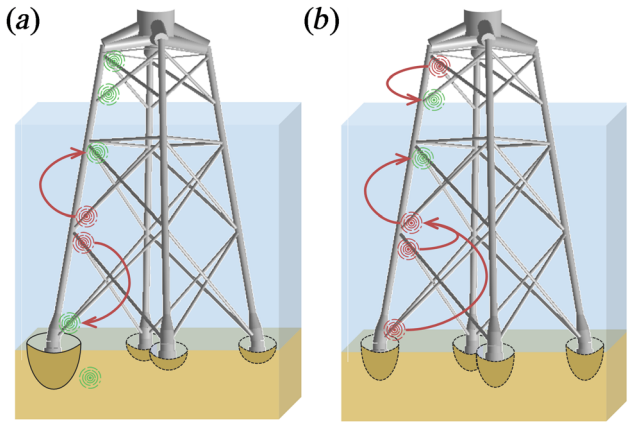

Fig. 11 Illustration of the detection algorithm capability—trained on frequencies and the $\bar{\delta}_j$ –, to locate (*a*) each anomaly scenarios for slight variations of scour depth and (*b*) the integrity loss of brace members for local scour depths close to the design allowance

5 Toward Field Applicability: Challenges and Limitations

The results, shown and discussed in Sec. 4, prove the feasibility of the suggested approach for the detection and location of failure events in the jacket substructure of the offshore wind turbine. The steps to set-up the monitoring strategy outlined in Fig. 1 are achieved in the matter of the training of a detection algorithm on the simulated data. The trained model fulfills the criteria of (i) diagnostic capability, (ii) low-cost—as opposed to any other ad hoc monitoring system and field inspections, (iii) transparency of reasoning process, as required for the industrial needs delineated in Sec. 1.3. As concerns the eventual use of this probabilistic model for the decision making of maintenance actions (iv), the fuzzy clustering method allows to judge the prediction for the membership of the data to all the possible classes. However, this will be not as easy to interpret for the real-time data and the raising of alarms. Instead, it should be considered to make an engineering judgment on the evolution of the predictions in time. The implementation for real-time field monitoring, and (v) requires, as a next step, to verify the accuracy of its predictions on a set of data from the real structure.

Some of the challenges of dealing with modal data extracted from field measurements—especially in the case of offshore wind structures—come from their scatter and fluctuation in time caused by complex loads and rotating mass. As a first step one could apply the detection algorithm on only the data from the idling turbine—as done here –, when the excitations and the inoperability of the turbine have less of an impact on the methods for the extraction of the modal properties. Alternatively, the extracted modal properties can be preprocessed, by filtering mode shapes that do not satisfactorily match with the analytical modes of the FE-updated model. By setting a suitable threshold on the distance—either in terms of MAC value or as combination of frequency difference and MAC value—between the extracted and the analytical modes, some of the scatter in the data would be removed without losing important information for the detection algorithm.

However, it must be noted that this filtering procedure as well the lack of excitation, and thus poor OMA performance, can quite often lead to a lack of some required modes. In this respect, multiple detection models should be setup for adapting the prediction to the varying number of features available. This approach and the likely drop in accuracy caused by the removal of modes in the training phase are yet to be investigated.

6 Conclusions and Future Work

This study demonstrates the feasibility of the identification of damage scenarios and their location based on the tracking of the modal properties for an offshore wind jacket structure. The approach suggested is based on the training of an unsupervised fuzzy clustering algorithm, after having applied a supervised features transformation technique (i.e., LDA), on a reduced set of data, for obtaining the maximum separability of the clusters. The detection scheme fulfills the identified needs in low-cost equipment, transparency, probabilistic output and low computational effort for real-time monitoring and decision support.

The results from applying the trained algorithm on a validation datasets show the correct detection of all the anomalies, with promising capabilities to identify the location of the brace integrity loss. The healthy status and extreme scour scenarios are always classified correctly. Additionally, the brace disconnection-damage are always classified as such. Best damage location capabilities are seen by combining frequencies and $\bar{\delta}_j$ as training features, followed by the combination of MAC and frequencies. The frequencies-only detection show the most mistaken results as concerns the location of the anomalies. A summary of the damage location capability of the best feature combination is further visualized in Fig. 11. Each anomaly is indicated with a circular

sign, colored in green if the location is correctly identified, and in red otherwise (cf. the color version of the figure). The arrows are then used to point to the mistaken location of the damage. It can be seen that a good identification of the location of the damaged brace is possible for small variations of scour depth—Fig. 11(*a*). A mistaken identification of the damage location, however, is likely for higher scour depth variations—Fig. 11(*b*). Yet, it is worth noticing that the algorithm correctly distinguishes the damage locations between above and below the water level.

It should be noted that the detection strategy suggested in this paper can be applied to any offshore wind substructure type, as long as all information and processes required for the detection—cf. Sec. 2.1—are available. The monitoring has been setup to detect mutually exclusive failure events, by applying a multiclass classification approach. This decision is justified by the relatively young age of the structure. In the first years of life of the offshore wind turbine, such failures can be caused either by the misjudgement of the field conditions or by unexpected events. This method can be replaced by a multilabel setup in the long run, when the support structure is more likely to be affected by multiple failure events (e.g., by reaching the scour allowance, while corrosion progressively develops on the jacket braces).

Further challenges for the field application of the detection algorithms will come from the statistical uncertainty of the measured data, associated with the OMA and the violation of the method's assumptions for the extraction of modal parameters [17,18,52]. When the aim is to track the evolution and deviation of the modal properties, it is necessary to verify whether the deviation due to the presence of an anomaly is bigger than scatter in the data. This is the focus of ongoing research on the applicability and validation of this method for a real system.

Funding Data

- European Union's Horizon 2020 (Grant No. 745625; Funder ID: H2020-LCE-2016-RES-IA).
- University of Strathclyde (Grant No. EP/L016303/1; Funder ID: 10.13039/100008078).

References

[1] Fischer, K., and Coronado, D., 2015, "Condition Monitoring of Wind Turbines: State of the Art, User Experience and Recommendations," VGB PowerTech, **2015**(7), pp. 51–56.

[2] Cevasco, D., Koukoura, S., and Kolios, A. J., 2021, "Reliability, Availability, Maintainability Data Review for the Identification of Trends in Offshore Wind Energy Applications," Renewable Sustainable Energy Rev., **136**, p. 110414.

[3] Fischer, K., Pelka, K., Puls, S., Poech, M.-H., Mertens, A., Bartschat, A., Tegtmeier, B., Broer, C., and Wenske, J., 2019, "Exploring the Causes of Power-Converter Failure in Wind Turbines Based on Comprehensive Field-Data and Damage Analysis," Energies, **12**(4), p. 593.

[4] Luo, H., 2017, "Physics-Based Data Analysis for Wind Turbine Condition Monitoring," Clean Energy, **1**(1), pp. 4–22.

[5] Tautz-Weinert, J., and Watson, S. J., 2017, "Using SCADA Data for Wind Turbine Condition monitoring - A Review," IET Renewable Power Gener., **11**(4), pp. 382–394.

[6] Stetco, A., Dinmohammadi, F., Zhao, X., Robu, V., Flynn, D., Barnes, M., Keane, J., and Nenadic, G., 2019, "Machine Learning Methods for Wind Turbine Condition Monitoring: A Review," Renewable Energy, **133**, pp. 620–635.

[7] Herring, R., Dyer, K., Martin, F., and Ward, C., 2019, "The Increasing Importance of Leading Edge Erosion and a Review of Existing Protection Solutions," Renewable Sustainable Energy Rev., **115**(September), p. 109382.

[8] Scheu, M. N., Tremps, L., Smolka, U., Kolios, A., and Brennan, F., 2019, "A Systematic Failure Mode Effects and Criticality Analysis for Offshore Wind Turbine Systems Towards Integrated Condition Based Maintenance Strategies," Ocean Eng., **176**(October 2018), pp. 118–133.

[9] Rubert, T., Zorzi, G., Fusiek, G., Niewczas, P., McMillan, D., McAlorum, J., and Perry, M., 2019, "Wind Turbine Lifetime Extension Decision-Making Based on Structural Health Monitoring," Renewable Energy, **143**(May), pp. 611–621.

[10] Lian, J., Cai, O., Dong, X., Jiang, Q., and Zhao, Y., 2019, "Health Monitoring and Safety Evaluation of the Offshore Wind Turbine Structure: A Review and Discussion of Future Development," Sustainability (Switzerland), **11**(2), p. 494.

[11] Rolfes, R., Tsiapoki, S., and Häckell, M. W., 2014, "Sensing Solutions for Assessing and Monitoring Wind Turbines," *Sensor Technologies for Civil Infrastructures*, 1st ed., Elsevier, pp. 565–604.

[12] Avci, O., Abdeljaber, O., Kiranyaz, S., Hussein, M., Gabbouj, M., and Inman, D. J., 2021, "A Review of Vibration-Based Damage Detection in Civil Structures: From Traditional Methods to Machine Learning and Deep Learning Applications," Mech. Syst. Signal Process., **147**, p. 107077.

[13] Martinez-Luengo, M., Kolios, A., and Wang, L., 2016, "Structural Health Monitoring of Offshore Wind Turbines: A Review Through the Statistical Pattern Recognition Paradigm," Renewable Sustainable Energy Rev., **64**, pp. 91–105.

[14] Tcherniak, D., Chauhan, S., and Hansen, M. H., 2011, "Applicability Limits of Operational Modal Analysis to Operational Wind Turbines," Struct. Dyn. Renewable Energy, **1**(July), pp. 317–327.

[15] Tcherniak, D., Carcangiu, C. E., and Rossetti, M., 2012, "Application of OMA to Operational Wind Turbine: Methods for Cleaning Up the Campbell Diagram," Noise and Vibration Engineering 2012, ISMA 2012, including USD 2012: International Conference on Uncertainty in Structure Dynamics, Leuven, Belgium, Sept. 17–19, Vol., 6, pp. 4435–4446.

[16] Oliveira, G., Magalhães, F., Cunha, Á., and Caetano, E., 2018, "Vibration-Based Damage Detection in a Wind Turbine Using 1 Year of Data," Struct. Control Health Monit., **25**(11), p. e2238.

[17] Dong, X., Lian, J., Yang, M., and Wang, H., 2014, "Operational Modal Identification of Offshore Wind Turbine Structure Based on Modified Stochastic Subspace Identification Method Considering Harmonic Interference," J. Renewable Sustainable Energy, **6**(3), p. 033128.

[18] Dong, X., Lian, J., Wang, H., Yu, T., and Zhao, Y., 2018, "Structural Vibration Monitoring and Operational Modal Analysis of Offshore Wind Turbine Structure," Ocean Eng., **150**(92), pp. 280–297.

[19] Tcherniak, D., and Larsen, G. C., 2013, "Application of OMA to an Operating Wind Turbine: Now Including Vibration Data From the Blades," 5th International Operational Modal Analysis Conference, IOMAC 2013, Guimarães, Portugal, May 13–15, pp. 1–12.

[20] Weijtjens, W., Verbelen, T., Sitter, G. D., and Devriendt, C., 2016, "Foundation Structural Health Monitoring of an Offshore Wind Turbine—A Full-Scale Case Study," Struct. Health Monit., **15**(4), pp. 389–402.

[21] Weijtjens, W., Verbelen, T., Capello, E., and Devriendt, C., 2017, "Vibration Based Structural Health Monitoring of the Substructures of Five Offshore Wind Turbines," Procedia Eng., **199**, pp. 2294–2299.

[22] Oliveira, G., 2016, "Structural Health Monitoring of Wind Turbines," Faculdade de engenharia, Universidade do Porto, Porto, Portugal.

[23] Johnson, R. A., and Wichern, D. W., 2013, *Applied Multivariate Statistical Analysis* Prentice Hall, Upper Saddlle River, NJ.

[24] Rytter, A., 1993, *Vibrational Based Inspection of Civil Engineering Structures*, Aalborg University, Aalborg, Denmark.

[25] Tatsis, K. E., Agathos, K., Chatzi, E. N., and Dertimanis, V. K., 2022, "A Hierarchical Output-Only Bayesian Approach for Online Vibration-Based Crack Detection Using Parametric Reduced-Order Models," Mech. Syst. Signal Process., **167**(PB), p. 108558.

[26] Ou, Y., Tatsis, K. E., Dertimanis, V. K., Spiridonakos, M. D., and Chatzi, E. N., 2021, "Vibration-Based Monitoring of a Small-Scale Wind Turbine Blade Under Varying Climate Conditions. Part I: An Experimental Benchmark," Struct. Control Health Monit., **28**(6), pp. 1–18.

[27] Nguyen, C. U., Lee, S. Y., Kim, H. T., and Kim, J. T., 2019, "Vibration-Based Damage Assessment in Gravity-Based Wind Turbine Tower Under Various Waves," Shock Vib., **2019**, pp. 1–17.

[28] Richmond, M., Smolka, U., and Kolios, A., 2020, "Feasibility for Damage Identification in Offshore Wind Jacket Structures Through Monitoring of Global Structural Dynamics," Energies, **13**(21), p. 5791.

[29] Nguyen, C., Huynh, T., and Kim, J., 2018, "Vibration-Based Damage Detection in Wind Turbine Towers Using Artificial Neural Networks," Struct. Monit. Maint., **5**(4), pp. 507–519.

[30] Duvnjak, I., Damjanović, D., Bartolac, M., and Skender, A., 2021, "Mode Shape-Based Damage Detection Method (Msdi): Experimental Validation," Appl. Sci. (Switzerland), **11**(10), p. 4589.

[31] Lu, Q., Ren, G., and Zhao, Y., 2002, "Multiple Damage Location With Flexibility Curvature and Relative Frequency Change for Beam Structures," J. Sound Vib., **253**(5), pp. 1101–1114.

[32] Ratcliffe, C. P., and Bagaria, W. J., 1998, "Vibration Technique for Locating Delamination in a Composite Beam," AIAAJ, **36**(6), pp. 1074–1077.

[33] Wang, Y., Liang, M., and Xiang, J., 2014, "Damage Detection Method for Wind Turbine Blades Based on Dynamics Analysis and Mode Shape Difference Curvature Information," Mech. Syst. Signal Process., **48**(1–2), pp. 351–367.

[34] Liu, K., Yan, R. J., and Soares, C. G., 2018, "Damage Identification in Offshore Jacket Structures Based on Modal Flexibility," Ocean Eng., **170**(October), pp. 171–185.

[35] Alvandi, A., and Cremona, C., 2006, "Assessment of Vibration-Based Damage Identification Techniques," J. Sound Vib., **292**(1–2), pp. 179–202.

[36] Malekzehtab, H., and Golafshani, A. A., 2013, "Damage Detection in an Offshore Jacket Platform Using Genetic Algorithm Based Finite Element Model Updating With Noisy Modal Data," 2nd International Conference on Rehabilitation and Maintenance in Civil Engineering, Solo, Indonesia, Mar. 8–10, Vol. 54, pp. 480–490.

[37] Xu, M., Wang, S., and Li, H., 2019, "A Residual Strain Energy Based Damage Localisation Method for Offshore Platforms Under Environmental Variations," Ships Offshore Struct., **14**(7), pp. 747–754.

[38] Diao, Y., Men, X., Sun, Z., Guo, K., and Wang, Y., 2018, "Structural Damage Identification Based on the Transmissibility Function and Support Vector Machine," Shock Vib., **2018**, pp. 1–13.

[39] Cheng, Y. S., and Wang, Z., 2008, "Detecting Damage to Offshore Platform Structures Using the Time-Domain Data," J. Mar. Sci. Appl., **7**(1), pp. 7–14.
[40] Wagg, D. J., Worden, K., Barthorpe, R. J., and Gardner, P., 2020, "Digital Twins: State-of-the-Art and Future Directions for Modeling and Simulation in Engineering Dynamics Applications," ASCE-ASME J. Risk Uncertainty Eng. Syst., Part B: Mech. Eng., **6**(3), pp. 1–17.
[41] Worden, K., Cross, E. J., Barthorpe, R. J., Wagg, D. J., and Gardner, P., 2020, "On Digital Twins, Mirrors, and Virtualizations: Frameworks for Model Verification and Validation," ASCE-ASME J. Risk Uncertainty Eng. Syst., Part B: Mech. Eng., **6**(3), pp. 1–9.
[42] Tygesen, U. T., Jepsen, M. S., Vestermark, J., Dollerup, N., and Pedersen, A., 2018, "The True Digital Twin Concept for Fatigue Re-Assessment of Marine Structures," Proc. Int. Conf. Offshore Mech. Arct. Eng. - OMAE, **1**(June)
[43] Augustyn, D., Smolka, U., Tygesen, U. T., Ulriksen, M. D., and Sørensen, J. D., 2020, "Data-Driven Model Updating of an Offshore Wind Jacket Substructure," Appl. Ocean Res., **104**(May), p. 102366.
[44] Pastor, M., Binda, M., and Harčarik, T., 2012, "Modal Assurance Criterion," MMaMS, **48**(48), pp. 543–548.
[45] Pandey, A. K., and Biswas, M., 1994, "Damage Detection in Structures Using Changes in Flexibility," J. Sound Vib., **169**(1), pp. 3–17.
[46] Li, T., Zhu, S., and Ogihara, M., 2006, "Using Discriminant Analysis for Multi-Class Classification: An Experimental Investigation," Knowl. Inf. Syst., **10**(4), pp. 453–472.
[47] Suganya, R., and Shanthi, R., 2012, "Fuzzy C-Means Algorithm-A Review," Int. J. Sci. Res. Publ., **2**(11), pp. 2250–3153.
[48] Fuzzy c-Means, 2015, More than one cluster center [Online]. Available at: http://researchhubs.com/post/ai/fundamentals/fuzzy-c-means.html#:~text=Advantages%3A [Accessed: March, 11 2021].
[49] Warner, J. D., and "Fuzzy Logic SciKit (Toolkit for SciPy)," accessed Mar. 10, 2021, https://github.com/scikit-fuzzy/scikit-fuzzy
[50] Scikit-Learn 0.22 Online Guide - 3.1. "Cross-Validation: Evaluating Estimator Performance - 3.1.2.2.1. Stratified k-Fold".
[51] NGI Group, 2017, "BSEE Offshore Wind Recommendations - Guidlines for Structural Health Monitoring for Offshore Wind Turbine Towers and Foundations,"
[52] Weinert, J., Smolka, U., Schümann, B., and Cheng, P. W., 2015, "Detecting Critical Scour Developments at Monopile Foundations Under Operating Conditions," Proceedings of the European Wind Energy Association Annual Event, EWEA 2015, Paris, France, Nov. 17–20, pp. 135–139.
[53] Ferri, C., Hernández-Orallo, J., and Modroiu, R., 2009, "An Experimental Comparison of Performance Measures for Classification," Pattern Recognit. Lett., **30**(1), pp. 27–38.